

## Factors controlling sea salt abundances in the urban atmosphere of a coastal South American megacity

Marina Dos Santos<sup>a,b,c</sup>, Laura Dawidowski<sup>b,c,d</sup>, Patricia Smichowski<sup>a,b</sup>, Ana Graciela Ulke<sup>e,f</sup>, Darío Gómez<sup>b,c,d,\*</sup>

<sup>a</sup> Consejo Nacional de Investigaciones Científicas y Técnicas (CONICET), Av. Rivadavia 1917, C1033AAJ Buenos Aires, Argentina

<sup>b</sup> Comisión Nacional de Energía Atómica, Gerencia Química, Av. Gral. Paz 1499, B1650KNA-San Martín, Pcia. de Buenos Aires, Argentina

<sup>c</sup> Universidad de San Martín, Instituto de Investigación e Ingeniería Ambiental, Argentina, Peatonal Belgrano 356, San Martín, Buenos Aires, Argentina

<sup>d</sup> Universidad de Buenos Aires, Facultad de Ingeniería, Departamento de Ingeniería Química, Ciudad Universitaria, Buenos Aires, Argentina

<sup>e</sup> Universidad de Buenos Aires, Facultad de Ciencias Exactas y Naturales, Departamento de Ciencias de la Atmósfera y los Océanos, Pab. II, 2do Piso, C1428EGA Buenos Aires, Argentina

<sup>f</sup> Unidad Mixta Internacional, Instituto Franco Argentino sobre Estudios de Clima y sus Impactos (IFAECI)/CNRS, Argentina

### H I G H L I G H T S

- ▶ Sea salt is always present in PM<sub>2.5</sub> and PM<sub>2.5–10</sub> of the Buenos Aires aerosol.
- ▶ Oceanic influence under local and regional meteorological conditions is ratified.
- ▶ The ratio  $\{[\text{Cl}^-]+[\text{Mg}^{2+}]+[\text{Na}^+]\}/\text{PM}$  best expresses variability in sea salt levels.
- ▶ Simple mathematical tools provide robust results to characterize sea salt patterns.
- ▶ Significant Cl<sup>-</sup> depletion was registered from both, PM<sub>2.5</sub> and PM<sub>2.5–10</sub>.

### A R T I C L E I N F O

#### Article history:

Received 22 December 2011

Received in revised form

8 May 2012

Accepted 11 May 2012

#### Keywords:

Marine aerosols

Sea salt chemical markers

Sodium chloride

Chloride depletion

Back-trajectory analysis

Buenos Aires

Argentina

### A B S T R A C T

The South Atlantic oceanic influence in the ambient air of Buenos Aires was studied on the basis of the measured concentrations of Cl<sup>-</sup>, Mg<sup>2+</sup> and Na<sup>+</sup>, as chemical markers of marine aerosols. A total of 113 fine (PM<sub>2.5</sub>) and 113 coarse (PM<sub>2.5–10</sub>) samples were collected over a one-year period in an inland sampling site located ~250 km from the open sea and ~7.5 km from the shore of the La Plata River, which flows into the Atlantic Ocean. The ratio  $r_{\text{ion-PM}}$  between the added concentrations of the three ions and the corresponding aerosol mass concentration was also used as a sea salt indicator. The behavior of these indicators under various meteorological conditions was used to identify and characterize the presence of sea salt in the urban aerosol. The influence of regional meteorological conditions was assessed by means of the Potential Source Contribution Function (PSCF) while that of local conditions was assessed by categorized percentile distributions analysis. The pattern of the PSCF for different ranges of the four sea salt indicators, exhibiting a transition from lowest values under continental influence to highest values under oceanic influence, provided robust evidence that the marine aerosol from the South Atlantic Ocean reaches the city of Buenos Aires. The  $r_{\text{ion-PM}}$  ratio, which combines the opposite effects of wind speed on the aerosol mass and ion concentrations, was identified as the most sensitive indicator of sea salt aerosol variations. Percentile distributions of the  $r_{\text{ion-PM}}$  ratio, disaggregated according to onshore (NE, E, SE, S) and offshore (N, NW, W, SW) winds and speeds above and below the median (4.3 m s<sup>-1</sup>), clearly indicated that the highest levels of marine aerosol occurred under onshore winds and wind speeds > 4.3 m s<sup>-1</sup>. In addition to characterizing the oceanic influence in Buenos Aires, we reported the expected sea salt levels under different conditions and estimated the magnitude of chloride depletion. This is the first study on sea salt levels in the urban atmosphere of this coastal megacity that reports and makes available a set of consistent concentrations of marine aerosol markers measured over a one-year period.

© 2012 Elsevier Ltd. All rights reserved.

### 1. Introduction

The primary marine aerosol is produced by wind stress at the ocean surface resulting in the mechanical generation of sea-spray aerosol (O'Dowd and de Leeuw, 2007). Sea salt consists

\* Corresponding author. Comisión Nacional de Energía Atómica, Gerencia Química, Av. Gral. Paz 1499, B1650KNA-San Martín, Pcia. de Buenos Aires, Argentina. Tel.: +54 11 6772 7130; fax: +54 11 6772 7886.

E-mail address: [dgomez@cnea.gov.ar](mailto:dgomez@cnea.gov.ar) (D. Gómez).

predominantly of chlorine (Cl) and sodium (Na) and carries also other chemical elements (Millero, 2004). Sea salt aerosol (SSA) plays an important role in many physical and chemical atmospheric processes at urban, regional and global scales. It influences radiative transfer directly by scattering solar radiation and indirectly by forming cloud condensation nuclei (CCN) and increasing cloud-top reflectivity (Yoon and Brimblecombe, 2002). When the halogens that are bound in the atmospheric particles are released to the atmosphere they play a significant role in atmospheric chemistry by intervening in a number of chemical reactions. Chlorine may be mobilized from SSA by: (i) the release of gaseous hydrochloric acid (HCl) through the reaction of sodium chloride (NaCl) with gaseous acids, particularly nitric or sulphuric acids ( $\text{HNO}_3$ ,  $\text{H}_2\text{SO}_4$ ); (ii) the formation of gaseous dichloride ( $\text{Cl}_2$ ) through reactions of hydroxyl ( $\text{OH}^-$ ) with  $\text{Cl}^-$  at the air water interface of deliquesced NaCl; and (iii) heterogeneous reactions at the surface of SSA, especially with nitrogen oxides that can promote the release of compounds such as nitrosyl chloride (ClNO) (Finlayson-Pitts, 2003; von Glasow, 2008).

The chlorine species released to the atmosphere from SSA take part of the inorganic halogen chemistry, which is closely intertwined with the complex chemical cycles that form and remove ozone from the troposphere (Finlayson-Pitts, 2003). Osthoff et al. (2008) have recently identified nitryl chloride ( $\text{ClNO}_2$ ), mainly produced by the night-time reaction of dinitrogen pentoxide ( $\text{N}_2\text{O}_5$ ) with chloride containing aerosol as a key precursor for enhanced ozone formation after sunrise.

For air quality assessment in coastal areas, it is necessary to take into account the large gradients in SSA levels along sea-inland directions. This feature is considered in a number of regional models, which include a description of sea salt. However, the verification of these models is severely hampered by the limited number of available ground-based measurements worldwide (Manders et al., 2010). This scarcity of data may be associated with the relatively low attention that air pollution researchers, traditionally more concerned with health impacts, have paid to the relatively benign SSA (White, 2008). Despite this situation, recent studies in Europe and the United States compiled measurements of concentrations of sea salt markers in aerosols collected in a significant number of ground-based monitoring sites. Manders et al. (2010) compiled Na concentrations measured in 89 sites distributed in 16 European countries to assess the spatial variability of sea salt concentrations and to provide a basis for the validation of a regional air quality model used to simulate sea salt distribution. White (2008) assessed the adequacy of using  $\text{Cl}^-$  as a SSA marker using the chemically speciated fine-particle concentrations measured at about 170 rural or remote sites from the IMPROVE network (interagency monitoring of protected visual environments) in the United States.

Assessments about the air quality situation of the metropolitan area of Buenos Aires (MABA) and other South American cities have also mostly overlooked SSA. In Buenos Aires, the city government operates an air pollution monitoring network, which reports carbon monoxide, nitrogen oxides and  $\text{PM}_{10}$ . Practically all information about  $\text{PM}_{2.5}$  in the MABA has been reported by researchers (e.g., Magallanes et al., 2008 and references therein). Only three of these studies have considered the concentration of  $\text{Na}^+$ ,  $\text{Cl}^-$  and other ions composing the SSA (Bogo et al., 2003; Magallanes et al., 2008; Dos Santos et al., 2009). Bogo et al. (2003) reported concentrations of eight ions in 30  $\text{PM}_{10}$  samples collected in Buenos Aires between December 1998 and September 1999; levels of  $\text{Cl}^-$  and  $\text{Na}^+$  were in the ranges  $3.9\text{--}6.7 \mu\text{g m}^{-3}$  and  $1.0\text{--}3.8 \mu\text{g m}^{-3}$ , respectively. The authors postulated a marine influence, based on the relatively high levels of  $\text{Cl}^-$  and  $\text{Na}^+$  when compared to reference levels in the United Kingdom. Magallanes et al. (2008) applied a new multivariate analysis technique to a set of ion profiles of 18

$\text{PM}_{10}$  samples. They identified three clusters; one of them contained the three samples with the highest  $\text{Cl}^-$  and  $\text{Na}^+$  concentrations associated with back-trajectories mostly over the South Atlantic Ocean. Dos Santos et al. (2009) reported the concentration of 12 elements and four ions measured in 226 samples collected during a one-year monitoring campaign. The authors identified significant correlations in  $\text{PM}_{2.5-10}$  (soluble fraction) of  $\text{Cl}^-$  with  $\text{Na}^+$  and Mg and indicated that  $\text{Na}^+$  and  $\text{Cl}^-$  were predominantly associated with  $\text{PM}_{2.5-10}$ . Although these studies reported valuable data about the ionic species present in the local aerosol, they did not advance in analyzing the role of SSA in the atmosphere of Buenos Aires.

This paper presents an analysis of the concentrations of chemical sea salt markers ( $\text{Cl}^-$ ,  $\text{Mg}^{2+}$  and  $\text{Na}^+$ ), measured by Dos Santos et al. (2009). It provides information on the distribution of sea salt in  $\text{PM}_{2.5}$  and  $\text{PM}_{2.5-10}$  in the MABA and examines the main local and regional meteorological conditions associated with sea salt abundances in the local urban atmosphere. The concentrations of ions analyzed constitute a unique set of ground-based observational data that together with the associated SSA estimates and, possibly combined with ship-based measurements, may be useful for the verification of regional transport models in areas influenced by the South Atlantic Ocean.

## 2. Studied area

The MABA is composed by the city of Buenos Aires ( $34^\circ 38'S$ ,  $58^\circ 28'W$ ) and 24 neighboring districts (Fig. 1a). It has a surface of  $\sim 3800 \text{ km}^2$  and a population of  $\sim 16$  million, which ranks it as the 11th megacity in the world and the third in Latin America. The MABA is located on the southern shore of the La Plata river (Río de la Plata), which has a funnel shape;  $\sim 300 \text{ km}$  in length, oriented northwest to southeast. The limit between the Río de la Plata and the Atlantic Ocean has been defined as the line joining Punta del Este, Uruguay ( $34^\circ 58.5' S$ ,  $54^\circ 57.5' W$ ) and Cabo San Antonio, Argentina ( $36^\circ 18' S$ ,  $56^\circ 46' W$ ) (Fig. 1b).

The estuary is characterized by high susceptibility to atmospheric forcing because of its large extension and shallow water depth. Guerrero et al. (1997) have characterized the seasonal influence of wind pattern on surface salinity distribution, with spring–summer dominated by onshore winds (NE, E, SE, and S), and fall–winter characterized by a balance between onshore and offshore winds (N, NW, W, and SW). For our purpose, the upriver marine influence may be simply characterized by the isolines of 5–10 su (salinity units, as reported by Guerrero et al., 1997) and the outer zone with salinity between 25 and 30 su (Fig. 1b).

Local climate is under the influence of the seasonal behavior of the semi-permanent systems, particularly, the subtropical South Atlantic anticyclone (SAA) and synoptic and mesoscale events, such as fronts and convective storms. Air moisture has high values throughout the year, with a slight increase in winter. The prevailing wind directions are in the NE to S sector, due to the influence of the SAA and the coastal location, during most of the year.

Air pollution potential in the Buenos Aires air shed was characterized in climatological studies in terms of mixing height and ventilation factor (Ulke and Mazzeo, 1998; Ulke, 2004). The estimated mean daytime mixing heights are 936 m in summer and 457 m in winter, and the annual mean is 695 m. These values are smaller than the critical one (1500 m) indicative of a reduced boundary layer for pollutants' dilution. The moderate intensities of wind speed translate to the mean ventilation factors, which are  $11,000 \text{ m}^2 \text{ s}^{-1}$  in summer and  $5500 \text{ m}^2 \text{ s}^{-1}$  in winter. The probabilities of reduced ventilation are 71% in winter and 55% on an annual basis.

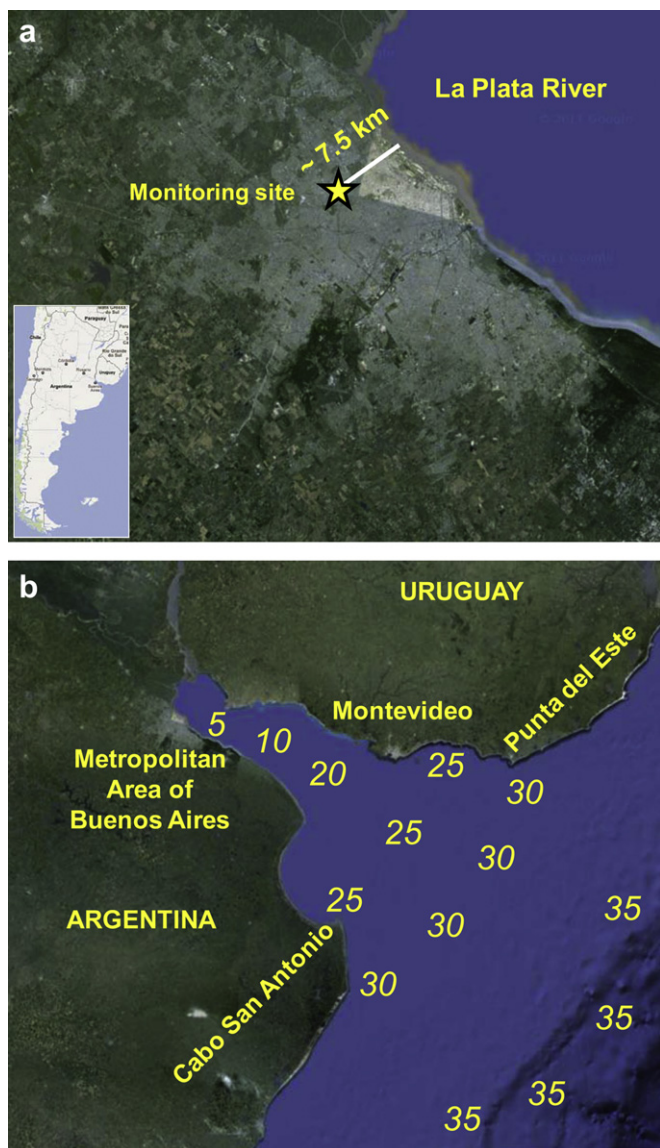


**Fig. 1.** (a) The monitoring site in the urban sprawl of the metropolitan area of Buenos Aires. (b) Estuary of the La Plata River. The imaginary line between Cabo San Antonio (Argentina) and Punta del Este (Uruguay) indicates the limit between the river and the Atlantic Ocean. The river's surface salinity gradient is represented by the values of salinity units (su) between 5 and 35, based on Guerrero et al. (1997).

### 3. Materials and methods

Sections 3.1–3.3 summarize experimental aspects regarding sampling and analytical determinations. For further information the reader is referred to the study by Dos Santos et al. (2009).

#### 3.1. Sample collection and fractionation

The collection of airborne particulate matter was carried out during one year from October 2005 to October 2006 at one sampling site on the roof of a building at Comisión Nacional de Energía Atómica (34° 38'S, 58° 28'W) located at ~15 m distance from a highway and at ~12 m above the ground level. It is at approximately 250 km from the open sea and 7.5 km from the shore of the Río de la Plata. It is mainly influenced by emissions from residential sources and urban vehicular traffic. A total of 113 coarse (PM<sub>2.5–10</sub>) and 113 fine (PM<sub>2.5</sub>) samples were collected using a Gent

sampler equipped with a stacked filter unit (Maenhaut et al., 1993). The collection time per sample was normally 24 h to collect an aerosol mass sufficient for analytical determinations. Each filter was placed in a clean polyethylene bag during transport and storage.

#### 3.2. Sample treatment

The aerosol mass was obtained by weighing each filter before and after sampling under controlled temperature and humidity conditions. Subsequently, the samples were subjected to a 2-step leaching procedure. In the first step, the soluble components were extracted using the procedure described by Dos Santos et al. (2009). These filtrates were used for the determination of water-soluble anions, cations, metals and metalloids. The characterization of the chemical components of aerosol was completed with the analysis of metals and metalloids in the non-soluble fractions.

#### 3.3. Analytical determination

Ions were identified and determined in the water-soluble extracts by High Performance Liquid Chromatography (HPLC) employing a Konik (Barcelona, Spain) KNK-500A liquid chromatograph equipped with a Rheodyne (Cotati, CA, USA) Model 7125 injector, a 100 µl sample loop and analytical columns; a conductimetric detector was used in all cases. Data were processed by means of integration software, Konikrom Chromatography Data System V.5 (Barcelona, Spain). For anions separation and determination by HPLC a Hamilton PRP-X100 column (polystyrene-divinylbenzene; 25 cm × 4.1 mm; id. 10 µm) was used. The mobile phase was a 4.5 mM potassium hydrogen phthalate solution (Merck) at a pH of 4.5. For cations separation and determination by HPLC a Wescan Cations Standard analytical column was selected. A 3 mM nitric acid solution (Merck) at pH 2.5 was employed as mobile phase.

Determination of Mg along with other 11 trace elements was carried out by Inductively Coupled Plasma Optical Emission Spectrometry (ICP OES) using a Perkin–Elmer (Norwalk, CT USA) ICP Optima 3100 XL (axial view) provided with a Model AS 90 auto-sampler. All measurements were performed by triplicate and the reported results are averaged values.

Selection of the monitoring site, operation, treatment and handling of samples and data validation were carried out according to QA/QC guidelines of the World Health Organization.

#### 3.4. Data analysis

To elucidate the oceanic influence in the urban atmosphere of Buenos Aires, we assessed the behavior of sea salt markers under local and regional meteorological conditions. To this end, we considered the use of Cl<sup>-</sup>, Mg<sup>2+</sup> and Na<sup>+</sup> concentrations as chemical sea salt markers. Concentrations of Mg<sup>2+</sup> correspond to the concentrations of Mg determined by ICP OES in the soluble fraction of the PM samples. In addition, we also considered the ratio  $r_{\text{ion-PM}}$  between the mass concentration of these three ions and the overall aerosol mass concentration as an alternative sea salt marker (Eq. (1)).

$$r_{\text{ion-PM}} = \frac{[\text{Cl}^-] + [\text{Mg}^{2+}] + [\text{Na}^+]}{\text{PM}} \quad (1)$$

For each size fraction (PM<sub>2.5</sub> or PM<sub>2.5–10</sub>), the variables were compiled in a 113 × 5 matrix (113 samples times (1 mass concentration + 3 ions (Cl<sup>-</sup>, Na<sup>+</sup>, Mg<sup>2+</sup>) +  $r_{\text{ion-PM}}$  ratio)). Best fitting distribution for each element concentration was assessed by means

of Quantile–Quantile (Q–Q) plots. Correlations between measured concentrations were analyzed through correlation matrices and scatter plots of all possible pairs.

The influence of regional conditions on the selected sea salt markers was assessed using the Potential Source Contribution Function (PSCF), defined below. Percentile analysis (Croxford and Penn, 1998) was used to assess the variability of these markers with seasons and local meteorological conditions namely, 16 wind directions and average values of wind speed and relative humidity over the sampling period. To perform this analysis, the original set of  $113 \times 5$  set of measured concentrations was expanded with the meteorological variables. The final data set was a  $113 \times 23$  matrix of physical, chemical and meteorological variables. Hourly values of wind direction, wind speed and relative humidity measured at Aeroparque ( $34^{\circ}34'S$ ,  $58^{\circ}30'W$ ), (close to the Río de La Plata), were provided by the National Weather Service of Argentina.

The Potential source contribution function represents a quantification of the potential of a source area to cause elevated aerosol concentrations at a specified receptor site (Malm et al., 1986). For our study, the PSCF combines the measured composition data of  $Cl^-$ ,  $Mg^{2+}$  and  $Na^+$  and the calculated  $r_{ion-PM}$  ratio with air parcel back-trajectories, to incorporate regional meteorological information into a receptor model analysis. We evaluated PSCFs over a geographical area delimited by  $70^{\circ}S$ ,  $125^{\circ}W$  and  $0^{\circ}$ ,  $30^{\circ}W$ , which was divided in grid cells of  $1^{\circ} \times 1^{\circ}$ . The PSCF value for a given grid cell is calculated by counting the trajectory segment endpoints within that grid cell. PSCF is defined in Eq. (2) in terms of the total number of endpoints  $n(i, j)$  that fall in the cell  $i, j$  during the overall measuring period of all collected samples, and the subset  $m(i, j)$  of these endpoints that arrived at the sampling site under specified conditions.

$$PSCF(i, j) = \frac{m(i, j)}{n(i, j)} \quad (2)$$

For each selected sea salt marker, we calculated four PSCF( $i, j$ ) corresponding to the quartiles of its distribution. In the PSCF analysis, small values of  $n(i, j)$  can produce high PSCF values (1) with high uncertainty. In order to minimize this artifact we identified those cases with PSCF( $i, j$ ) = 1 and  $n(i, j)$  = 1, 2, 3 and reported them separately, to avoid generalization over a limited number of cases.

Three-day backward three-dimensional trajectories were calculated using the Hybrid Single-Particle Lagrangian Integrated Trajectory model (HYSPPLIT\_4) developed at the National Oceanic and Atmospheric Administration – Air Resources Laboratory (NOAA ARL, USA), (Draxler and Hess, 1997). The Final Run (FNL)-Southern Hemisphere (SH) Archive furnished by NOAA ARL was used as the meteorological input to HYSPPLIT4.9. The information is provided at 0000, 0600, 1200, 1800 UTC (Coordinated Universal Time), at the surface and 13 mandatory pressure levels. For each sampling period, 72-h back-trajectories arriving at the collection site every 6 h and covering the entire period were obtained.

A computer program was developed to process the back-trajectories data and calculate the PSCFs ( $i, j$ ) of interest, which were saved in a matrix. A pictorial representation of the information provided by the PSCF is shown in Fig. 2, which is discussed hereinbelow.

We have estimated sea salt mass concentrations in air using two different estimators. The simplest approach (Eq. (3)), introduced by Manders et al. (2010), indicates that  $Na^+$  is 30.6% of total sea salt mass concentration.

$$[\text{sea salt}] = 3.26 [Na^+] \quad (3)$$

Marenco et al. (2006) took into account the combined contribution of  $Cl^-$  and  $Na^+$  and other ionic constituents (Eq. (4)) that

account for 14% of sea salt. Their contribution is expressed in terms of  $Na^+$  concentration as a factor of 0.46 (0.14/0.306).

$$[\text{sea salt}] = 1.46 [Na^+] + [Cl^-] \quad (4)$$

#### 4. Results and discussion

Mean mass concentrations were  $6.2 \mu\text{g m}^{-3}$  for  $PM_{2.5}$  and  $13.8 \mu\text{g m}^{-3}$  for  $PM_{2.5-10}$  and mean concentrations of the sea salt chemical markers ( $Na^+$ ,  $Cl^-$  and  $Mg^{2+}$ ) were respectively 0.44, 0.72 and  $0.11 \mu\text{g m}^{-3}$  in the coarse fraction and 0.26, 0.22 and  $0.044 \mu\text{g m}^{-3}$  in the fine fraction. The annual mean  $PM_{10}$  concentration in our study was much lower than that measured by our group in 2001 ( $64.5 \mu\text{g m}^{-3}$ ) (Dos Santos et al., 2009 and references therein) but compatible with the annual mean concentration registered in 2010 ( $38 \mu\text{g m}^{-3}$ ), which has been reported by the Environmental Protection Agency of Buenos Aires. The  $PM_{2.5-10}$  and  $PM_{2.5}$  data from our one-year measuring campaign were the only time-series of these two fractions available for us. These data are not enough to postulate the reasons for the relatively low concentration levels obtained. The main statistical features of the concentrations measured in this study are reported in Table 1 while the entire data set is reported in an Annex, as supplementary material. As sea salt is typically more abundant in the coarser aerosol fraction (O'Dowd and de Leeuw, 2007), the following analysis of the results focuses in the  $PM_{2.5-10}$  fraction.

##### 4.1. Sea salt presence in the Buenos Aires $PM_{2.5-10}$

All measured concentrations were adequately fitted by right-skewed distributions. For this reason, both the mean and the median are reported in Table 1, since the last one is a better indication of the central tendency of the data. In many samples, especially  $PM_{2.5}$  samples, the concentrations of one or more of the three sea salt markers were below the corresponding limit of detection (LOD):  $Cl^-$  ( $0.192 \mu\text{g m}^{-3}$ ),  $Mg^{2+}$  ( $0.0075 \mu\text{g m}^{-3}$ ),  $Na^+$  ( $0.096 \mu\text{g m}^{-3}$ ). In these cases, to avoid bias towards higher concentration values in estimating the statistical parameters, a value equal to half the corresponding LOD was assigned to the concentrations lying below these limits (Polisar et al., 1998). Several studies have indicated increasing inland concentrations of SSA under increasing wind speed; although this increasing profile is highly dependent on wind direction (Morcillo et al., 2000; Wai and Tanner, 2004; O'Dowd and de Leeuw, 2007). Table 2 provides an overall picture of the variability of  $PM_{2.5-10}$ ,  $Cl^-$ ,  $Mg^{2+}$  and  $Na^+$  concentrations and  $r_{ion-PM}$  values with wind speed. It is clearly evident that  $PM_{2.5-10}$  concentration decreases as wind speed increases while sea salt markers exhibit the opposite behavior. This increasing profile of  $Cl^-$ ,  $Mg^{2+}$  and  $Na^+$  concentrations and  $r_{ion-PM}$  with wind velocity is consistent with the mentioned behavior of SSA and constitutes the first indication in our study of sea salt presence in the Buenos Aires aerosol.

Regional oceanic influence was assessed by means of the Potential Source Contribution Function for  $Cl^-$ ,  $Mg^{2+}$  and  $Na^+$  concentrations and  $r_{ion-PM}$ . The values for each variable were organized according to their quartile distribution. For each variable, we calculated four PSCFs corresponding to the four quartiles, amounting to a total of 16 PSCFs. The four sets of PSCFs corresponding to the selected sea salt markers exhibit in general a similar behavior, which is exemplified in Fig. 2 for  $r_{ion-PM}$ , which was later identified as the best sea salt indicator.

The set of four PSCFs depicted in Fig. 2 provides evidence that the marine aerosol from the South Atlantic Ocean reaches the MABA. PSCF distributions exhibit a clear transition from that

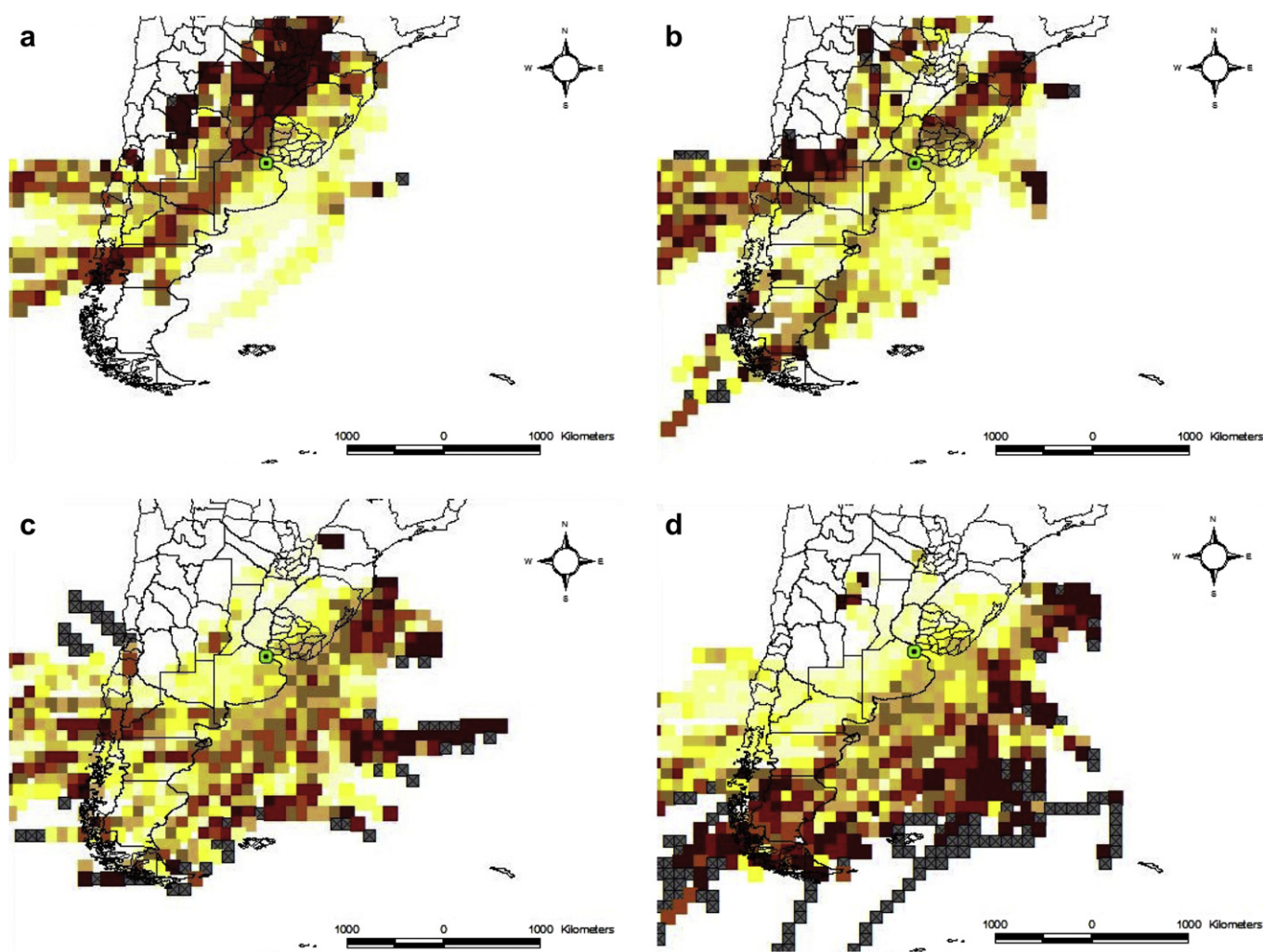


**Fig. 2.** Potential Source Contribution Function (PSCF), defined in Eq. (2) for the four quartiles of the  $r_{\text{ion-PM}_{2.5-10}}$  ratio (defined in Eq. (1)). (a) First quartile ( $0 \leq r_{\text{ion-PM}_{2.5-10}} < 0.027$ ). (b) Second quartile ( $0.027 \leq r_{\text{ion-PM}_{2.5-10}} < 0.065$ ). (c) Third quartile ( $0.065 \leq r_{\text{ion-PM}_{2.5-10}} < 0.16$ ). (d) Fourth quartile ( $0.16 \leq r_{\text{ion-PM}_{2.5-10}} < 0.4$ ). PSCF( $i, j$ ) values are depicted in a color scale corresponding to the ranges indicated below.  $< 0.11$ ;  $0.11-0.16$ ;  $0.16-0.21$ ;  $0.21-0.26$ ;  $0.26-0.32$ ;  $0.32-0.38$ ;  $0.38-0.46$ ;  $0.46-0.54$ ;  $0.54-0.71$ ;  $0.71-1.0$ ;  $= 1$  and  $n(i, j) \leq 3$ . Legends for the color figure to be reproduced in color on the Web:  $< 0.11$ ;  $0.11-0.16$ ;  $0.16-0.21$ ;  $0.21-0.26$ ;  $0.26-0.32$ ;  $0.32-0.38$ ;  $0.38-0.46$ ;  $0.46-0.54$ ;  $0.54-0.71$ ;  $0.71-1.0$ ;  $= 1$  and  $n(i, j) \leq 3$ . (For interpretation of the references to colour in this figure legend, the reader is referred to the web version of this article.)

belonging to the first quartile (Fig. 2.a) to that belonging to the fourth quartile (Fig. 2.d). The PSCF for the lowest  $r_{\text{ion-PM}}$  values is clearly dominated by continental back-trajectories with a noticeable presence of those from the N–NE direction. On the other hand, the PSCF belonging to the highest  $r_{\text{ion-PM}}$  values exhibits almost exclusively the influence of oceanic back-trajectories. The

intermediate PSCFs belonging to the second and third quartiles show the transition from continental to oceanic influence.

The  $r_{\text{ion-PM}}$  ratio was identified as the most sensitive indicator of sea salt based on the cumulative PSCF values for four characteristic regions that were defined as continental and oceanic, subdivided as North, South with  $35^{\circ}\text{S}$  (South of Buenos Aires city) as the limit. The continental region encompasses Argentina, Uruguay and the part of Brazil depicted in Fig. 2. Chile, on the West, was not considered in this study because of the topographic barrier imposed by the Andes Mountains. Cumulative PSCFs values exhibit a similar behavior for the four sea salt markers, indicating a clear transition of the highest values from North continental (first quartile) to South oceanic (fourth quartile) regions. However, for the cumulative PSCFs values for  $r_{\text{ion-PM}}$  exhibit the largest range and variability between regions. Another feature indicated in Table 3 is that for the third quartile, the cumulative values of PSCF of the North oceanic region are, for all markers, the largest ones. Therefore, the influence of the North oceanic region on the marine aerosol in Buenos Aires is relatively more noticeable for the sea salt marker values belonging to the third quartile of the distribution. It is plausible to postulate that the  $r_{\text{ion-PM}}$  ratio is the most sensitive indicator of sea salt aerosol

**Table 1**

Descriptive statistics of measured concentrations ( $\mu\text{g m}^{-3}$ ) of sea salt tracers for  $\text{PM}_{2.5}$  and  $\text{PM}_{2.5-10}$  samples collected in Buenos Aires.

	$\text{Na}^+$	$\text{Mg}^{2+}$	$\text{Cl}^-$	Aerosol mass
$\text{PM}_{2.5}$				
Minimum	0.05	0.003	0.096	0.2
Median	0.09	0.024	0.096	5.8
Mean	0.19	0.05	0.23	6.17
Maximum	5.31	1.04	4.14	16.2
$\text{PM}_{2.5-10}$				
Minimum	0.05	0.004	0.096	1.3
Median	0.24	0.062	0.426	12.8
Mean	0.44	0.11	0.73	13.78
Maximum	2.63	2.25	3.20	39.6

**Table 2**  
Distribution of chemical sea salt markers ( $\text{Na}^+$ ,  $\text{Cl}^-$  and  $\text{Mg}^{2+}$ ) and  $r_{\text{ion-PM}_{2.5-10}}$  values with frequency distribution of wind speed.

Wind intensity distribution		$\text{PM}_{2.5-10}$ mean ( $\mu\text{g m}^{-3}$ )	$\text{Cl}^-$ mean ( $\mu\text{g m}^{-3}$ )	$\text{Mg}^{2+}$ mean ( $\mu\text{g m}^{-3}$ )	$\text{Na}^+$ mean ( $\mu\text{g m}^{-3}$ )	$r_{\text{ion-PM}_{2.5-10}}$ <sup>a</sup> mean
Quartile	Mean ( $\text{m s}^{-1}$ )					
Q1	< 3.46	2.63	19.49	0.37	0.06	0.22
Q2	3.46–4.34	3.93	13.93	0.58	0.08	0.33
Q3	4.34–5.26	4.78	11.37	0.98	0.08	0.54
Q4	> 5.26	6.42	10.29	0.97	0.10	0.70

<sup>a</sup> Defined in Eq. (1).

variations because it is the only one that combines the opposite effects of wind speed on the concentrations of  $\text{Cl}^-$ ,  $\text{Mg}^{2+}$  and  $\text{Na}^+$  and  $\text{PM}_{2.5-10}$ , summarized in Table 2.

The seasonal behavior of SSA under local meteorological conditions namely, wind speed, wind direction and relative humidity, was analyzed by means of percentile analysis of the frequency distribution of the different sea salt chemical markers. Wind data were organized according to onshore (NE, E, SE, S) and offshore (N, NW, W, SW) directions according to the line perpendicular to the major axis of the La Plata River (Guerrero et al., 1997). Wind speed was classified in two sets above and below the median ( $4.3 \text{ m s}^{-1}$ ). As in the assessment based on PSCFs, the results for the four markers were similar and therefore we concentrate the following discussion on the  $r_{\text{ion-PM}}$ . No major differences were appreciated in the percentile distribution for the different seasons and for different relative humidity levels. Contrariwise, percentile distribution under different wind directions and speeds exhibited significant variability. Percentile distributions of the  $r_{\text{ion-PM}}$  ratio, disaggregated according to these two parameters, are depicted in Fig. 3 together with the overall percentile distribution. The percentile distribution under onshore winds and wind speeds higher than  $4.3 \text{ m s}^{-1}$  is clearly differentiated from the rest of the distributions, including the overall one. It indicates the highest occurrence of high  $r_{\text{ion-PM}}$  values throughout the whole distribution. The distribution under offshore winds and wind speeds below  $4.3 \text{ m s}^{-1}$  indicates the highest occurrence of low values. The distributions for the other two parameter combinations lie closer to the overall distribution and in general below it. This analysis helps

to identify the conditions under which relatively high sea salt concentrations may be expected in the urban atmosphere of Buenos Aires.

In Fig. 4, scatter plots of the measured concentrations of  $\text{Cl}^-$ ,  $\text{Na}^+$  and  $\text{Mg}^{2+}$  are compared with the corresponding  $\text{Cl}^-/\text{Na}^+$ ,  $\text{Cl}^-/\text{Mg}^{2+}$  and  $\text{Mg}^{2+}/\text{Na}^+$  ratios documented for sea water (Millero, 2004). This comparison was done to elucidate whether the sea salt markers considered in this study were predominantly derived from sea salt or there were other significant contributors over Buenos Aires. The best fits for the measured data for the  $\text{Cl}^-:\text{Na}^+$  and  $\text{Cl}^-:\text{Mg}^{2+}$  pairs corresponded to quadratic functions while the pair  $\text{Mg}^{2+}:\text{Na}^+$  was best fitted by a linear function. For the  $\text{Cl}^-$ ,  $\text{Na}^+$  pair the best fitting quadratic approximation became, at low concentrations, practically tangent to the  $\text{Cl}^-/\text{Na}^+$  ratio in sea water. For  $[\text{Na}^+] > 0.5 \mu\text{g m}^{-3}$ ,  $\text{Cl}^-$  concentrations were on average lower than the corresponding values in sea water. These two features, depicted in Fig. 4.a, provide evidence that (i)  $\text{Na}^+$  in  $\text{PM}_{2.5-10}$  determined in this study mainly derived from sea salt and (ii) the existence of significant  $\text{Cl}^-$  depletion in the measured data, which was noticeable only under onshore winds. The best fit for the measured  $\text{Cl}^-$ ,  $\text{Mg}^{2+}$  concentrations was practically parallel to the  $\text{Cl}^-/\text{Mg}^{2+}$  ratio for  $[\text{Mg}^{2+}] < 0.1 \mu\text{g m}^{-3}$  (Fig. 4b). The non-zero x-intercept at  $[\text{Mg}^{2+}] = 0.02 \mu\text{g m}^{-3}$  ( $\sim 2.5 \text{ LOD}$ ) may be attributed to a source of  $\text{Mg}^{2+}$ , other than sea salt. Another well-known Mg source is the earth crust; however it is unlikely that this source be significantly contributing to the soluble fraction of Buenos Aires  $\text{PM}_{2.5-10}$ . The geological sources of this metal are most likely contributing to the non-soluble fraction, which accounted for  $\sim 80\%$  of the total Mg in

**Table 3**  
Cumulative values of the Potential Source Contribution Functions (PSCFs)Eq. (1), for each quartile of the distributions of the concentrations of  $\text{Cl}^-$ ,  $\text{Mg}^{2+}$  and  $\text{Na}^+$  in  $\text{PM}_{2.5-10}$  and the  $r_{\text{ion-PM}_{2.5-10}}$  ratio, disaggregated according to four geographical regions. Latitude  $35^\circ\text{S}$  delimitates the North and South portions of the continental and oceanic areas considered.

Quartiles	First	Second	Third	Fourth
$\text{Na}^+$				
Continental North	0.39	0.33	0.29	0.14
Continental South	0.18	0.39	0.21	0.26
Oceanic North	0.21	0.18	0.55	0.32
Oceanic South	0.16	0.30	0.38	0.44
$\text{Mg}^{2+}$				
Continental N	0.52	0.38	0.17	0.14
Continental S	0.28	0.25	0.25	0.24
Oceanic N	0.13	0.19	0.57	0.60
Oceanic S	0.11	0.24	0.50	0.43
$\text{Cl}^-$				
Continental N	0.52	0.33	0.36	0.13
Continental S	0.19	0.33	0.24	0.30
Oceanic N	0.31	0.13	0.55	0.32
Oceanic S	0.12	0.24	0.36	0.52
$r_{\text{ion-PM}} = \{[\text{Na}^+] + [\text{Cl}^-] + [\text{Mg}^{2+}]\} / \text{PM}_{2.5-10}$				
Continental N	0.53	0.34	0.14	0.13
Continental S	0.32	0.29	0.23	0.24
Oceanic N	0.13	0.14	0.56	0.49
Oceanic S	0.11	0.20	0.40	0.56

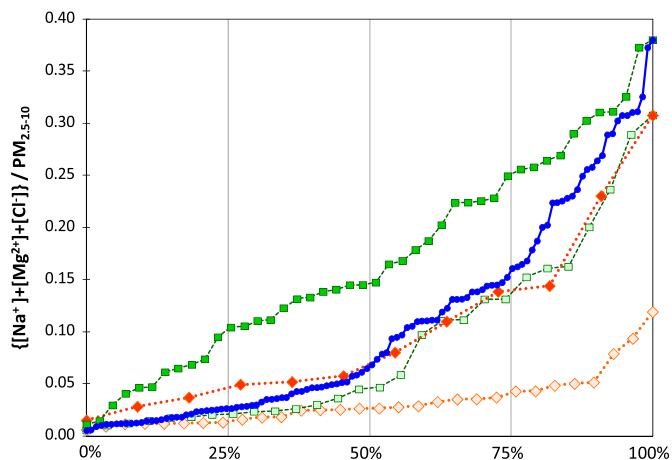


**Fig. 3.** Percentile distribution of  $r_{\text{ion-PM}_{2.5-10}}$  ratio (defined in Eq. (1)). —●— Overall distribution. —■— Onshore winds,  $v > 4.3 \text{ m s}^{-1}$ . - -■- Onshore winds,  $v < 4.3 \text{ m s}^{-1}$ . —◇— Offshore winds,  $v > 4.3 \text{ m s}^{-1}$ . - -◇- Offshore winds,  $v < 4.3 \text{ m s}^{-1}$ . Legends for the color figure to be reproduced in color on the Web: —●— Overall distribution. —■— Onshore winds,  $v > 4.3 \text{ m s}^{-1}$ . - -■- Onshore winds,  $v < 4.3 \text{ m s}^{-1}$ . —◇— Offshore winds,  $v > 4.3 \text{ m s}^{-1}$ . - -◇- Offshore winds,  $v < 4.3 \text{ m s}^{-1}$ . (For interpretation of the references to colour in this figure legend, the reader is referred to the web version of this article.)

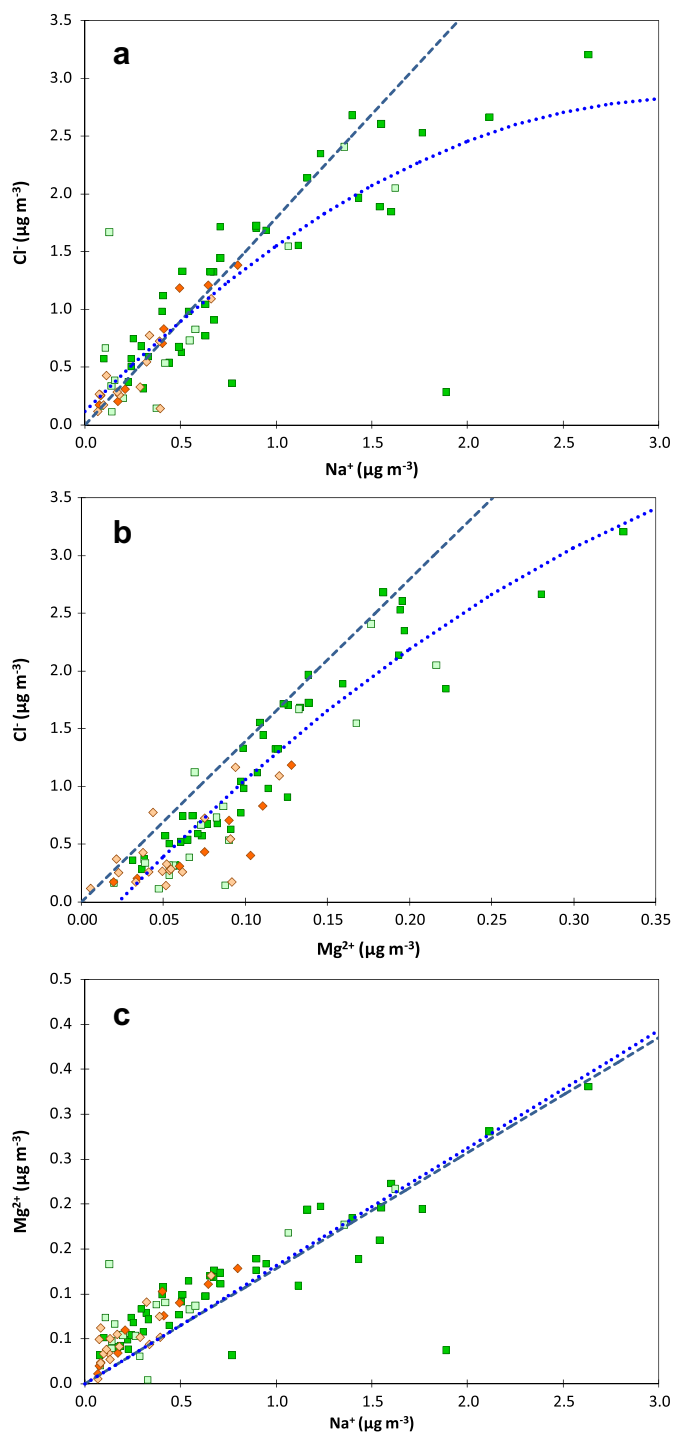


**Fig. 4.** Scatter plot of measured concentrations of  $\text{Cl}^-$ ,  $\text{Na}^+$  and  $\text{Mg}^{2+}$  in  $\text{PM}_{2.5-10}$ . The straight dashed line represents the relationship of the ions in sea water (Millero, 2004). The dotted line represents the best fit, represented by a quadratic function ( $r = 0.8$ ) in cases (a), (b) and by a linear function ( $r = 0.7$ ) in case (c). (a)  $\text{Cl}^-$  versus  $\text{Na}^+$ . (b)  $\text{Cl}^-$  versus  $\text{Mg}^{2+}$ . (c)  $\text{Mg}^{2+}$  versus  $\text{Na}^+$ .  $\blacksquare$  Onshore winds,  $v > 4.3 \text{ m s}^{-1}$   $\square$  Onshore winds,  $v < 4.3 \text{ m s}^{-1}$   $\blacklozenge$  Offshore winds,  $v > 4.3 \text{ m s}^{-1}$   $\blacklozenge$  Offshore winds,  $v < 4.3 \text{ m s}^{-1}$ . Legends for the color figure to be reproduced in color on the Web:  $\blacksquare$  Onshore winds,  $v > 4.3 \text{ m s}^{-1}$   $\square$  Onshore winds,  $v < 4.3 \text{ m s}^{-1}$   $\blacklozenge$  Offshore winds,  $v > 4.3 \text{ m s}^{-1}$   $\blacklozenge$  Offshore winds,  $v < 4.3 \text{ m s}^{-1}$ . (For interpretation of the references to colour in this figure legend, the reader is referred to the web version of this article.)

these samples (Dos Santos et al., 2009). Moreover, the parallelism between the trend and the  $\text{Cl}^-/\text{Mg}^{2+}$  ratio and the relative small value of the x-intercept are indicative that the trend is dominated by the sea salt contribution. Fig. 4b also shows decreasing levels of

the measured  $\text{Cl}^-$  as compared to those belonging to the sea water reference and provides further evidence of significant  $\text{Cl}^-$  depletion under onshore winds. In Fig. 4c, the slope of the trend line of the measured  $\text{Mg}^{2+}$  and  $\text{Na}^+$  concentrations practically coincides with the ratio of these cations in sea salt, confirming that they are predominantly derived from this origin. Most data points with  $[\text{Mg}^{2+}] < 0.2 \text{ } \mu\text{g m}^{-3}$  lie above the sea-salt ratio. This may be related to (i) the mentioned minor contribution of a different source of  $\text{Mg}^{2+}$  and (ii) the comparatively higher accuracy of the results provided by ICP OES, the analytical technique used for the quantification of Mg.

A preliminary estimate of  $\text{Cl}^-$  depletion relative to  $\text{Na}^+$  levels in the atmosphere of Buenos Aires is formulated in Eq. (5), as the difference between chloride concentration in sea water and the quadratic function of best fitting curve in Fig. 4a.  $\text{Mg}^{2+}$  was left out in Eq. (5) because of the likely contribution, albeit relatively small, of this metal by another source.

$$[\text{Cl}^-_{\text{depleted}}] = 0.267 [\text{Na}^+]^2 + 0.090 [\text{Na}^+] - 0.113 \quad (5)$$

All concentrations in Eq. (5) are in  $\mu\text{g m}^{-3}$  and the expression is valid for  $[\text{Na}^+] > 0.75 \text{ } \mu\text{g m}^{-3}$ .

#### 4.2. Sea salt presence in the Buenos Aires $\text{PM}_{2.5}$

We have also analyzed the possible presence of sea salt aerosol in the finer fraction of the collected samples. The largest difficulty to undertake this analysis is the large number of samples for which the concentrations of the sea salt chemical markers were below the corresponding limit of detection (LOD). Out of the 113 collected samples,  $\text{Na}^+$  concentrations were below the LOD reached with the technique used for measurements in 30 samples (equivalent to  $\sim 27\%$ );  $\text{Mg}^{2+}$  concentrations were below the LOD in four samples ( $\sim 4\%$ ), and  $\text{Cl}^-$  concentrations were below the LOD in 90 samples ( $\sim 80\%$ ). Under these circumstances we did not analyze the individual concentrations of  $\text{Cl}^-$ ,  $\text{Mg}^{2+}$  and  $\text{Na}^+$ . We have only considered their combination with  $\text{PM}_{2.5}$  using the corresponding  $r_{\text{ion-PM}}$  ratio in the context of the PSCF analysis. The set of four PSCF belonging to the different quartiles of the  $r_{\text{ion-PM}}$  ratio distribution exhibited a similar transition (from lowest  $r_{\text{ion-PM}}$  values and continental influence to highest  $r_{\text{ion-PM}}$  values and South Atlantic oceanic influence) than that depicted in Fig. 2 for  $\text{PM}_{2.5-10}$ . In spite of this similarity the transition pattern was somewhat blurred, which may be related to the higher number of samples with low concentrations of the chemical sea salt markers.

The same comparison between the measured concentrations of  $\text{Cl}^-$ ,  $\text{Na}^+$  and  $\text{Mg}^{2+}$  with the corresponding  $\text{Cl}^-/\text{Na}^+$  and  $\text{Cl}^-/\text{Mg}^{2+}$  ratios in SSA undertaken for  $\text{PM}_{2.5-10}$  was done for  $\text{PM}_{2.5}$  taken only into account the subset of samples for which the concentrations of the measured ions were above the corresponding LOD. The analysis produced similar results, with the only remarkable difference that there was no evident source of  $\text{Mg}^{2+}$  other than sea salt.  $\text{Cl}^-$  depletion was also evident in the finer fraction.

The similarity in the pattern distribution of PSCFs for  $\text{PM}_{2.5}$  and  $\text{PM}_{2.5-10}$  and between  $\text{Cl}^-/\text{Na}^+$  and  $\text{Cl}^-/\text{Mg}^{2+}$  ratios in the  $\text{PM}_{2.5}$  samples and in SSA confirm that the selected sea salt markers in the finer fraction also had an oceanic origin.

#### 4.3. Estimation of sea salt concentrations in Buenos Aires

Sea salt mass concentrations, estimated according to Eqs. (3)–(4), are summarized in Table 4 using the combinations of wind direction and wind speed employed in this study. For  $\text{PM}_{2.5-10}$ ,

**Table 4**  
Estimated sea salt concentrations ( $\mu\text{g m}^{-3}$ ) in  $\text{PM}_{2.5}$  and  $\text{PM}_{2.5-10}$  using Eq. (3) (Manders et al., 2010) and Eq. (4) (Marengo et al., 2006). The percentage contribution of SSA to the corresponding total mass concentration is also reported.

	Eq. (3)				Eq. (4)			
	SSA in $\text{PM}_{2.5}$		SSA in $\text{PM}_{2.5-10}$		SSA in $\text{PM}_{2.5}$		SSA in $\text{PM}_{2.5-10}$	
	$\mu\text{g m}^{-3}$	%	$\mu\text{g m}^{-3}$	%	$\mu\text{g m}^{-3}$	%	$\mu\text{g m}^{-3}$	%
Offshore winds, $v < 4.3 \text{ m s}^{-1}$	$0.40 \pm 0.3$	$5.4 \pm 4.5$	$0.54 \pm 0.5$	$3.1 \pm 2.2$	$0.28 \pm 0.1$	$3.7 \pm 2.3$	$0.52 \pm 0.5$	$2.9 \pm 2.0$
Offshore winds, $v > 4.3 \text{ m s}^{-1}$	$0.24 \pm 0.1$	$6.1 \pm 4.3$	$1.0 \pm 0.9$	$11.6 \pm 9.2$	$0.23 \pm 0.1$	$6.2 \pm 2.8$	$1.0 \pm 0.9$	$11.8 \pm 10.1$
Onshore winds, $v < 4.3 \text{ m s}^{-1}$	$0.56 \pm 0.5$	$8.5 \pm 7.2$	$1.2 \pm 1.4$	$7.6 \pm 7.2$	$0.37 \pm 0.2$	$5.8 \pm 3.7$	$1.1 \pm 1.3$	$7.6 \pm 8.0$
Onshore winds, $v > 4.3 \text{ m s}^{-1}$	$0.39 \pm 0.7$	$8.6 \pm 12.9$	$2.5 \pm 2.0$	$21.3 \pm 14.3$	$0.44 \pm 0.5$	$10.1 \pm 12.5$	$2.2 \pm 1.7$	$19.5 \pm 11.3$

practically the same results were obtained using either equation while the results for  $\text{PM}_{2.5}$ , although similar, exhibited some differences. The estimates of sea salt concentrations in  $\text{PM}_{2.5}$  are more uncertain because of the larger number of samples with  $\text{Cl}^-$  and  $\text{Na}^+$  concentrations below the LOD. For  $\text{PM}_{2.5-10}$ , expected sea salt concentration levels under onshore winds and wind speed  $> 4.3 \text{ m s}^{-1}$  are four times higher than those under offshore winds and wind speed  $< 4.3 \text{ m s}^{-1}$ . These values represent average percentage contributions of the SSA in  $\text{PM}_{2.5-10}$  of 20% and 3%, respectively. It can be noted that higher percentage of SSA are expected under higher wind speeds, even under offshore winds. As SSA levels are lower under offshore winds, the increase of the percentage contribution of SSA relates to the decrease of  $\text{PM}_{2.5-10}$  under higher wind speeds. Estimated percent SSA contributions to  $\text{PM}_{2.5}$  were between 4 and 5% (offshore winds,  $v < 4.3 \text{ m s}^{-1}$ ) and 9–10% (onshore winds,  $v > 4.3 \text{ m s}^{-1}$ ); however and unlike the situation for the coarse fraction, the estimated SSA concentrations exhibited similar levels under different wind conditions.

Through the analyses of our results in Sections 4.1–4.3, we have demonstrated that SSA was always present in the Buenos Aires aerosol, both in  $\text{PM}_{2.5}$  and  $\text{PM}_{2.5-10}$ . In the coarser fraction SSA concentrations were higher than in the finer fraction. Significant concentrations levels of SSA were registered in  $\text{PM}_{2.5-10}$ , particularly under onshore winds over  $4.3 \text{ m s}^{-1}$ . Sizable  $\text{Cl}^-$  depletion occurred from both,  $\text{PM}_{2.5}$  and  $\text{PM}_{2.5-10}$ , under onshore winds and different wind speeds. Consequently the released chlorine species may reach the atmosphere of the megacity and coexist with gaseous pollutants

emitted by stationary and mobile combustion sources in the urban area and by ship engine exhausts approaching and leaving the large Buenos Aires harbor. This finding coupled with the new perspective about the chlorine-mediated ozone production (von Glasow, 2008) raises particular concern in this coastal megacity.

#### 4.4. $\text{Na}^+$ concentrations in the atmosphere of Buenos Aires and other cities worldwide

Our monitoring point was located at approximately 250 km from the Ocean, as it is a single site we cannot assess how the sea salt aerosol profile varies with distance inland. To compensate for this drawback and also for comparative purposes, we considered our set of  $\text{Na}^+$  concentrations against the data for 75 cities worldwide collected from several studies (Mugica et al., 2009; Chow et al., 2002; Rastogi and Sarin, 2005; Gutiérrez-Castillo et al., 2005). Although we are aware of the limitations of gathering these data because of the differences in location, climate, sampling and analytical techniques, Fig. 5 indicates that on average the measured data are consistent with the general pattern of  $\text{Na}^+$  concentration–inland distance reported in the literature. Moreover, within the scarcity of data of sea salt chemical markers measured inland (Manders et al., 2010), our study provides a consistent set of concentrations of  $\text{Cl}^-$ ,  $\text{Mg}^{2+}$  and  $\text{Na}^+$  measured in a location which has not been covered thus far.

## 5. Conclusions

Our results confirmed the South Atlantic oceanic influence in the urban atmosphere of Buenos Aires. They allowed us to propose what can be regarded to some degree as climatology of the local sea salt aerosol, which identifies the main meteorological conditions influencing expected sea salt levels.

The concentrations of the three ions considered ( $\text{Cl}^-$ ,  $\text{Mg}^{2+}$  and  $\text{Na}^+$ ) resulted adequate sea salt chemical markers; however its combination with mass concentration by means of the  $r_{\text{ion-PM}}$  ratio proved to be the most sensitive indicator because it encompasses and expresses the opposite behavior of the concentrations of PM and sea salt tracers with wind speed.

We found out that the application of relative simple tools as PSCF and categorized percentile distribution provided robust results, which can be reproduced in a straightforward manner using the original data without the need for algebraic transformations.

In addition to characterizing the oceanic influence in Buenos Aires, we (i) reported the expected sea salt levels under different conditions; (ii) estimated the magnitude of chloride depletion; and (iii) confirmed the presence, albeit lower, of sea salt in  $\text{PM}_{2.5}$ .

Gaseous chlorine species released as a consequence of the detected  $\text{Cl}^-$  depletion in the Buenos Aires aerosol may affect the ozone production and destruction cycle in this large urban area where nitrogen oxides and aerosol chloride sources coexist.

Our study reports and makes available a consistent data set of concentrations of sea salt chemical markers measured over a one-

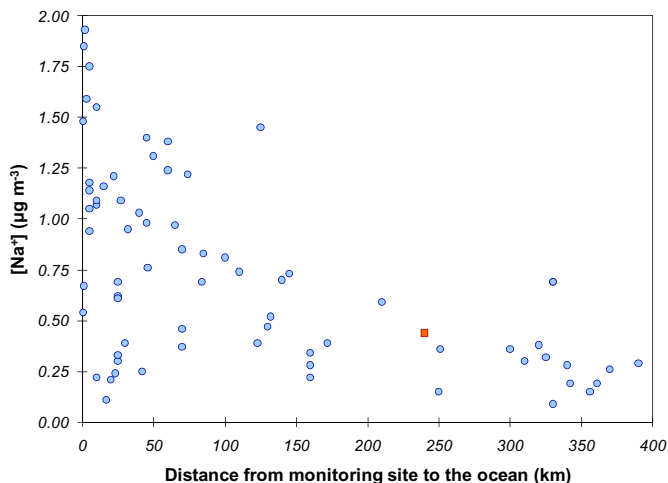


**Fig. 5.** Average  $\text{Na}^+$  concentrations versus distance to the sea in 76 cities worldwide.  $\square$  Concentrations measured in Buenos Aires (this study).  $\circ$  Compiled values of the concentrations measured in 75 cities of the following countries: Austria, Belgium, Denmark, Finland, Greenland, India, Italy, Lithuania, Mexico, the Netherlands, Norway, Slovakia, Spain, Switzerland and the United Kingdom (Mugica et al., 2009; Chow et al., 2002; Rastogi and Sarin, 2005; Gutiérrez-Castillo et al., 2005; Dos Santos et al., 2009).

year period in the coastal megacity of Buenos Aires, for which such information did not exist thus far.

### Acknowledgments

The authors acknowledge funding from the International Atomic Energy Agency (IAEA) through project RLA/7/011-ARCAL LXXX, the Agencia Nacional de Promoción Científica and Tecnológica through project PICT2008-1739, CONICET through Project PIP 486, the University of Buenos Aires through projects UBACYT IO33, X224 and 20020100101013 of Argentina and a grant from the Inter-American Institute for Global Change Research (IAI) CRN II 2017 which is supported by the US National Science Foundation (Grant GEO-0452325). We also thank the Servicio Meteorológico Nacional (National Weather Service of Argentina) for providing meteorological and climatological data. We are indebted with ARL/NOAA for the HYSPLIT model and the gridded meteorological fields. Fabián Fujiwara, Raquel Jasán, Rita Plá and Cristina Rössler are acknowledged for their kind cooperation.

### Appendix A. Supplementary material

Supplementary material related to this article can be found online at [doi:10.1016/j.atmosenv.2012.05.019](https://doi.org/10.1016/j.atmosenv.2012.05.019).

### References

- Bogo, H., Otero, M., Castro, P., Ozafrán, M.J., Kreiner, A., Calvo, E.J., Negri, R.M., 2003. Study of atmospheric particulate matter in Buenos Aires city. *Atmospheric Environment* 37, 1135–1147.
- Chow, J., Watson, J.G., Edgerton, S.A., Vega, E., 2002. Chemical composition of PM<sub>2.5</sub> and PM<sub>10</sub> in Mexico City during winter 1997. *Science of the Total Environment* 287, 177–201.
- Croxford, B., Penn, A., 1998. Siting considerations for urban pollution monitors. *Atmospheric Environment* 32, 1049–1057.
- Dos Santos, M., Gómez, D., Dawidowski, D., Gautier, E., Smichowski, P., 2009. Determination of water-soluble and insoluble compounds in size classified airborne particulate matter. *Microchemical Journal* 91, 133–139.
- Draxler, R.R., Hess, G.D., 1997. Description of the HYSPLIT\_4 Modelling System, NOAA Technical Memorandum ERL ARL-224, pp. 24.
- Finlayson-Pitts, B.J., 2003. The tropospheric chemistry of sea salt: a molecular-level view of the chemistry of NaCl and NaBr. *Chemistry Reviews* 103, 4801–4822.
- Guerrero, R.A., Acha, E.M., Frami, M.B., Lasta, C.A., 1997. Physical oceanography of the Río de la Plata Estuary, Argentina. *Continental Shelf Research* 17, 727–742.
- Gutiérrez-Castillo, M.E., Olivos-Ortiz, M., De Vizcaya-Ruiz, A., Cebrián, M.E., 2005. Chemical characterization of extractable water soluble matter associated with PM<sub>10</sub> from Mexico City during 2000. *Chemosphere* 61, 701–710.
- Maenhaut, W., François, F., Cafmeyer, J., 1993. The “GENT” Stacked Filter Unit (SFU) Sampler for the Collection of Atmospheric Aerosols in Two Size Fractions: Description and Instructions for Installation and Use. In: Report No. NAHRES-19. International Atomic Energy Agency, Vienna, pp. 249–263.
- Magallanes, J.F., Murruti, L., Gómez, D., Smichowski, P., Gettar, R., 2008. An Approach to air pollution source receptor solution by angular distances. *Water Air Soil Pollution* 188, 235–245.
- Malm, W.C., Johnson, C.E., Bresch, J.F., 1986. Application of principal component analysis for purposes of identifying source-receptor relationships. In: Pace, T.G. (Ed.), *Receptor Methods for Source Apportionment* No. TR-5. Air Pollution Control Association, Pittsburgh, PA.
- Manders, A.M.M., Schaap, M., Querol, X., Albert, M.F.M.A., Vercauteren, J., Kuhlbusch, T.A.J., Hoogerbrugge, R., 2010. Sea salt concentrations across the European continent. *Atmospheric Environment* 44, 2434–2442.
- Marengo, F., Bonasoni, P., Calzolari, F., Ceriani, M., Chiari, M., Cristofanelli, P., D'Alessandro, A., Fermo, P., Lucarelli, F., Mazzei, F., Nava, S., Piazzalunga, A., Prati, P., Valli, G., Vecchi, R., 2006. Characterization of atmospheric aerosols at Monte Cimone, Italy, during summer 2004: source apportionment and transport mechanisms. *Journal of Geophysical Research* 111 (24), art. No. D24202.
- Millero, F.J., 2004. Physicochemical controls on seawater. In: Holland, H.D., Turekian, K.K. (Eds.), *Treatise on Geochemistry*. Elsevier, Amsterdam (Chapter 6.01).
- Morcillo, M., Chico, B., Mariaca, L., Otero, E., 2000. Salinity in marine atmosphere corrosion: its dependence on the wind regime existing in the site. *Corrosion Science* 42, 91–104.
- Mugica, V., Ortiz, E., Molina, L., De Vizcaya-Ruiz, A., Nebot, A., Quintana, R., Aguilar, J., Alcántara, E., 2009. PM composition and source reconciliation in Mexico City. *Atmospheric Environment* 43, 5068–5074.
- O'Dowd, C.D., de Leeuw, G., 2007. Marine aerosol production: a review of the current knowledge. *Philosophical Transactions Royal Society A* 365, 1753–1774.
- Osthoff, H.D., Roberts, J.M., Ravishankara, A.R., Williams, E.J., Lerner, B.M., Sommariva, R., Bates, T.S., Coffman, D., Quinn, P.K., Dibb, J.E., Strak, H., Burkholder, J.B., Talukdar, R.K., Meagher, J., Fehsenfeld, F.C., Brown, S.S., 2008. High levels of nitryl chloride in the polluted subtropical marine boundary layer. *Nature Geoscience* 1, 324–328.
- Polisar, A.V., Paatero, P., Hopke, P.K., Malm, W.C., Sisler, J.F., 1998. Atmospheric aerosol over Alaska: 2. Elemental composition and sources. *Journal of Geophysical Research* 103, 19,045–19,057.
- Rastogi, N., Sarin, M.M., 2005. Long-term characterization of ionic species in aerosols from urban and high-altitude sites in western India: role of mineral dust and anthropogenic sources. *Atmospheric Environment* 39, 5541–5554.
- Ulke, A.G., Mazzeo, N.A., 1998. Climatological aspects of the daytime mixing height in Buenos Aires city, Argentina. *Atmospheric Environment* 32, 1615–1622.
- Ulke, A.G., 2004. Daytime ventilation conditions in Buenos Aires city, Argentina. *International Journal of Environment and Pollution* 22, 379–395.
- von Glasow, R., 2008. Pollution meets sea salt. *Nature Geoscience* 1, 292–293.
- Wai, K.M., Tanner, A., 2004. Wind-dependent sea salt aerosol in a Western Pacific coastal area. *Atmospheric Environment* 38, 1167–1171.
- White, W.H., 2008. Chemical markers for sea salt in IMPROVE aerosol data. *Atmospheric Environment* 42, 2319–2330.
- Yoon, Y.J., Brimblecombe, P., 2002. Modelling the contribution of sea salt and dimethyl sulfide derived aerosol to marine CCN. *Atmospheric Chemistry and Physics* 2, 17–30.